J. Membrane Biol. 71, 11–30 (1983)

The Journal of
Membrane Biology

Topical Review

Conduction and Selectivity in Potassium Channels

Ramon Latorre and Christopher Miller
Department of Physiology and Biophysics, Harvard Medical School, Boston, Massachusetts,
and Graduate Department of Biochemistry, Brandeis University, Waltham, Massachusetts

Introduction

A lipid bilayer membrane presents an enormous energy barrier to the movement of small ions. The electrostatic work required to transfer a K^+ ion, for example, from the aqueous medium of high dielectric constant to the interior of the low dielectric constant membrane is in the order of 250 kJ/mol (60 kcal/mol [119]). Because many cellular processes rely upon the passive diffusion of ions across biological membranes, a class of membrane proteins – the "ion channels" – has evolved to catalyze ion movements of this kind. Although the concept of the ion channel evolved from electrophysiological studies of ionic currents across the specialized membranes of nerve and muscle, it is now understood that these proteins are distributed widely throughout the biological world, appearing in membranes of prokaryotes, protozoa, and plant cells, as well as in nonexcitable animal cells of many types. Likewise, in addition to operating as the basis for the propagated electrical impulse of nerve and muscle membranes [69], ion channels are fundamentally involved in processes of hormone secretion [36, 37, 98], visual transduction [137], transepithelial electrolyte transport [90], contractile activation [54], and cell volume regulation [53].

Ion channels are integral membrane proteins spanning the lipid bilayer and necessarily communicating with both aqueous phases. Conceptually they may be considered as enzymes, in that they reduce the energies of transmembrane ionic diffusion from the 250 kJ/mol above to values in the range of 20 kJ/mol [44] – a rate enhancement of about 10^{39}. Hille [65] further pointed out that ion channels display the essential aspects of enzyme kinetics: saturation kinetics with substrate (ion) concentration, competitive inhibition by substrate analogues (blockers), and a tight substrate specificity (ionic selectivity). Beyond these characteristics of the ion-diffusion process itself, channels have the capability of undergoing rapid conformational changes between conducting ("open") and nonconducting ("closed") states. These opening and closing reactions can be driven by membrane potential, by the binding of chemical transmitters to receptors, and possibly by specific phosphorylation. None of these aspects of ion channel operation is unfamiliar in the literature of conventional enzymology.

But channels are unusual enzymes because of the extremely high absolute rates of catalysis they bring about, 10^6–10^9 ions transported per second, orders of magnitude higher than any other turnover rates known in biochemistry. Furthermore, the temperature dependence of these rates is generally very low ($Q_{10} \sim 1.2$–1.4, or 12–25 kJ/mol activation energy) [44]. Both the high transport rates and the low activation energies indicate that the diffusion pathway of these proteins must resemble a fixed hydrophilic pore involving energy barriers much smaller than those in which large changes in protein conformation occur in concert with the ion transport [9].

During the past ten years, the rates of ion movement through single channels have become accessible to direct measurement, through the use of three methods: the "macroscopic noise" technique [110], in which small fluctuations around a mean current due to many channels is analyzed; the "patch recording" methods [60, 109], in which unitary fluctuations of single channels are directly observed in a small area of cell membrane; and planar bilayer methods, in which "model channels" or biological membrane fragments are in-

Key words selectivity · ion-diffusion · channel structure · electrical excitation · excitable membranes

0022-2631/83/0071-0011 $04.00

serted into lipid bilayer membranes in which the single channel fluctuations may be directly observed [105]. We consider that enough data have now accumulated from these studies that it is possible to classify ion channels with respect to their conduction properties – that with few exceptions ion channels fall naturally into well-defined groups. It is the purpose of this review to illustrate this channel taxonomy, using those channels whose unitary conductance and ionic selectivity properties have both been characterized. We will then focus our discussion on two types of K^+ channels which may be discerned in these groupings: small, "classical" K^+ channels, and a newly recognized class of highly selective K^+ channels of very high conductance, which we call "maxi K^+ channels."

Taxonomy of Ion Channel Conduction and Selectivity

Ion channels have been regarded as molecular entities, rather than merely as "membrane processes," ever since the first direct observations of opening and closing of the "excitability-inducing material" (EIM) channel were made by Bean and co-workers [13] 15 years ago. Since that time, many channels have been subjected to detailed scrutiny, both "model channels," small peptides often of microbial origin, and, more recently, the integral membrane protein channels of higher organisms. Ion channels may be classified on the basis of their conduction and selectivity properties. The Table presents such a classification, using channels whose conductances and ionic sensitivities have been studied in some depth.

Intuitively, we would expect that the more selective a channel is, the lower its conductance should be. Increased selectivity requires an enhanced intimacy of the channel's interaction with the transported ions, an intimacy which in turn would seem to imply hindered diffusion for all ions. For example, Latorre et al. [83] established that the EIM channel has a very high unitary conductance (400 pS in 0.1 M KCl) and that the alkali metal cations permeate "nonselectively," in proportion to their free-solution mobilities. Likewise, Hille's [63] classic study of the selective Na^+ channel of frog node of Ranvier led to a picture of a region in the channel designed for strong, specific interactions with the Na^+ ion; this picture was in harmony with the early indications of a low conductance for this channel [27].

The Table distinguishes four classes of channels, and it is remarkable that virtually every channel which has been studied in enough detail to warrant inclusion in the Table falls quite naturally into one of these classes. The first group we term the "ion-selective channels," which not only distinguish ions according to electric charge, but also show substantial selectivity among ions of the same valence. The Na^+ and K^+ channels involved in action potential generation in nerve and muscle and the inward rectifier K^+ channels are the most familiar of these. A recently discovered Cl^--specific channel from *Torpedo* electroplax [106, 134] also belongs in this ion-specific group, as do highly selective Na^+ channels of amphibian epithelial apical membranes [16, 90, 118]. All of these channels have low conductance, on the order of 10 pS at 0.1 M salt, corresponding to net transport rates of about 10^6 ions per sec at 100 mV driving force.

A second group of "valence-selective channels" is well separated in behavior from the ion-selective channels. These channels are absolutely selective for ions of a given charge, but show little discrimination among ions of that charge. The best studied of these are the acetylcholine receptor (AchR) channel of the neuromuscular junction, and the gramicidin A (gram A) channel. Both of these exclude anions and allow monovalent cations to permeate. (The AchR channel also transports divalent cations.) Among the monovalent cations, however, there is rather little selectivity; in the AchR channel, for example, the monovalent cation permeabilities roughly parallel the ionic mobilities in free solution [12, 72]. For both of these channels, it may be presumed that anions are excluded by a nonspecific electrostatic barrier to entry into the channel and that, once inside, cations may diffuse in a largely unrestricted manner, with little specific interaction with the walls of the pore. This conclusion has been reached for the AchR channel on the basis of the large sizes of permeating organic cations [38, 72] and for gram A via an analysis of the rate constants of the various permeation steps [43] as well as from the known structure of the channel. In addition to these two intensely studied channels, there are many others which may be reasonably placed in the valence-selective group, including both anion- and cation-selective channels. All of these have higher conductances than those in the ion-selective group, in the range of 10^7 ions per sec, at 100 mV driving force.

We may discern a third group of "nonselective channels," with high conductance and little selectivity. With few exceptions, these channels allow all small ionic species to permeate, as well as nonelectrolytes. Channel conductances are roughly proportional to the electrical conductivity of the aqueous medium, in contrast to the more selective

Table. Ion channel conductance and selectivity

Channel	Preparation	Ionic condition[e]	γ, pS	Selectivity	Reference
A. Ion-specific channels					
Na^+ channel	Squid axon (*N*)	450 Na_o/50 Na_i	7	$Na^+(1) \sim Li^+ > K^+(0.09)$[x]	[27]
	Frog node (*N*)	105 Na_o/5 Na_i	8		
	Tunicate egg (*N*)	100 Na_o	3		[114]
	Rat muscle (*P*)	140 Na_o	18		[126]
	Frog skin (*N*)	60 Na_o	6	$Na^+(1) \sim Li^+ \gg Rb^+, K^+(0.001)$[y]	[16, 90, 118]
K^+ channel (delayed rectifier)	Squid axon (*N*)	10 K_o/400 K_i	12	$K^+(1) > Rb^+ > NH_4^+$ (0.3) $\gg Cs^+, Na^+ Li^+$[b]	[27]
	Squid axon (*P*)	460 K_o/1 K_i	18		[28]
	Squid axon (*T*)	400 K	3		[7]
	Frog node (*N*)	2.5 K_o/140 K_i	4	$Tl^+(2.3) > K^+(1) > Rb^+ > NH_4^+(0.13) \gg Na^+, Li^+$[b]	[64, 65]
	Helix neuron (*N*)	110 K	2	$Tl^+(1.3) > K^+(1) > Rb^+ > Cs^+ > Li^+ > Na^+(0.08)$[x]	[121]
K^+ channel (inward rectifier)	Frog muscle (*N*)	150 K_o	10		[125]
	Rat muscle (*P*)	150 K	10		[48, 116]
	Tunicate egg (*N*)	100 K_o/400 K_i	7	$Tl^+(1.5) > K^+(1) > Rb^+ > NH_4^+$ (0.04) $\gg Cs^+, Na^+, Li^+$[b]	[57]
	Tunicate egg (*P*)	50 K_o/400 K_i	5		[115]
K^+ channel (Ca^{2+}-activated)	Human erythrocyte (*P*)	100 K	18	$K^+ \gg Na^+$[b]	[59]
	Helix neuron (*P*)	4 K_o/400 K_i	19	$K^+ \gg Na^+$[b]	[92]
Cl^- channel	*Torpedo* electroplax (*B*)	150 Cl	9	$Cl^-(1) > Br^-(0.3) \gg I^-, F^-$[c]	[106, 134]
B. Valence-selective channels					
ElM	Bilayer	100 K	400	$Cs^+(1) > Rb^+ > K^+ > Na^+ > Li^+(0.4)$[c]	[40, 81]
Gramicidin A	Bilayer	100 Cs	15	$Cs^+(1) > Rb^+ > K^+ > Na^+ > Li^+(0.07)$[b]	[108]
Acetylcholine receptor	Frog muscle (*P*)	100 Na_o	35		[109]
	Rat muscle (*P*)	100 Na	40		[71]
	Rat muscle (*P*)	150 Na_o/150 K_i	35, 25[a]	$Cs^+ > K^+ > Na^+ > Li^+$ (0.7)[c]	[61]
	Torpedo electroplax (*B*)	100 Na	16		[112]
Glutamate receptor	Locust muscle (*P*)	200 Na_o	130	$K^+ \sim Na^+$[b]	[120]
Cation channel	Rat heart (*P*)	140 Na	35	$K^+ \sim Na^+$[b]	[26]
(Ca^{2+}-activated)	Neuroblastoma (*P*)	120 Na	22	$Cs^+ \sim K^+ \sim Na^+$[c]	[138]
Cation channel	Calf heart (*B*)	100 K	95	$K^+ \sim Na^+$[e]	[30]
Cation channel	Calf heart (*B*)	100 K	28	$K^+ > Na^+$ (0.2)[e]	[30]
Cation channel	Calf heart (*B*)	100 K	18	$K^+(1) > Na^+(0.3)$[e]	[30]
Anion channel	Bovine heart (*B*)	100 Cl	55	$Br^-(1) > Cl^- > I^- > F^-$ (0.4)[e]	[30, 35]
C. Nonselective channels					
Hemocyanin	Keyhole limpet (*B*)	100 K	200	$K^+(1) > Na^+ > Cl^- > Li^+$ (0.1)[e]	[24, 82, 99]
Porin	*E. coli* (*B*)	100 Na	140–480	None[d]	[18, 124]
Porin	Mitochondria (*B*)	100 K	450	None[d]	[25]
Alamethicin (state 5)	Bilayer	120 Na	630	None[d]	[41, 123]
D. Maxi-K^+ channels					
SR K^+ channel	Rabbit SR (*B*)	100 K	130	$K^+(1) > Rb^+ > Na^+ > Li^+(0.03)\ Cs^+$[c]	[34]
	Frog SR (*B*)	100	150,50[a]	$K^+(1) > Rb^+ > Na^+ > Li^+(0.07) \gg Cs^+$[c]	[80]
K^+ channel	Rabbit T-tubule (*B*)	100 K	230	$K^+(1) \gg Rb^+, Na^+, Li^+, Cs^+$[b]	[84]
(Ca^{2+}-activated)	Chromaffin cell (*P*)	140 K	180		[93]
	Rat myotubes (*P*)	140 K	187		[117]
	Rat pituitary (*P*)	145 K	208	$K^+ \gg Na^+$[b]	[135]
	Frog neuron (*P*)	2.5 K_o/100 K_i	100		[2]
	Rat axolemma (*B*)	100 K	230		[78]
	Rat muscle (*P*)	150 K	240		[100]

(*N*) Macroscopic noise method; (*P*) Patch method; (*B*) Planar bilayer method; (*T*) TEA-block method;
[a] Multiple open states;
[b] Selectivity determined from reversal potential.
[c] Selectivity determined from channel conductance.
[d] "None" indicates channels allowing permeation of molecules up to 500 molecular weight.
[e] Reported as concentration (in mM) of major conducting ion. Where no designation of internal or external concentration is given, symmetrical ionic conditions apply.

channels above, whose conductances saturate with ion concentration. In the case of mitochondrial porin [25], the channel size estimated from the cut-off size for permeating molecules agrees well with the size calculated from the channel conductance, assuming that ions diffuse through a pore of cylindrical geometry, with a conductivity equal to that of the aqueous medium. These hole sizes are calculated to be quite large, 20–30 Å in diameter, and the transport rates are enormous, 10^8–10^9 ions per sec, at 100 mV. Thus, these channels appear to operate simply as large water-filled holes punched through the membranes and will not be discussed here.

This review will discuss in some detail a fourth class of channels which departs egregiously from the intuitively satisfying conductance-selectivity behavior of the first three groups. These are all K^+-selective channels from animal cell membranes, they are all highly conductive, and they all were discovered during the past five years. These "maxi-K channels" have been observed by patch-recording methods in muscle [100, 117], chromaffin and pituitary cells [93, 135], and in neurons [2], and by planar bilayer techniques in sarcoplasmic reticulum [34, 79, 101], muscle plasma membranes [84], and brain plasmalemma preparations [78]. The striking property of these channels is that they greatly favor K^+ over other monovalent cations and absolutely exclude anions, as with the ion-selective category, but with conductances at 0.1 M K^+ of 130–200 pS, representing the transport of about 10^8 ions per sec at 100 mV, 10–50 times higher than rates of the ion-selective channels. There is clearly something unusual about these K^+ channels, and it is one purpose of this review to discuss them in relation to the conventional small K^+ channels and to point out what this anomalous behavior may have to say about their physical structures.

A review of the Table shows that many more types of K^+-selective channels are represented in the conductance-selectivity literature than is any other type of channel. For the remainder of this review, then, we will focus on conductance by K^+ channels, with the purpose of identifying crucial similarities and differences of the various K^+ channel types. We will see that the small K^+ channels of nerve and muscle, though long-studied, are quite complicated in their conduction behavior and therefore difficult to picture physically on the basis of electrical measurements. The maxi K^+ channels, in contrast, appear to be much simpler in operation, and therefore offer the hope of serving as models for developing a more precise view of ion channel architecture.

Small K^+ Channels: Are the Conduction Pathways Similar?

Delayed Rectifier

Conductance

This channel is responsible for the repolarization phase of the action potential and has been extensively characterized in both myelinated (frog) and nonmyelinated (squid) axons. In squid axon, macroscopic noise data yield values of channel conductance (12 pS) smaller than that obtained by measuring the channel amplitude directly (18 pS) (Table).

However, assuming that ion transport through the open K^+ channel follows the constant field equation, and taking into account the difference in ionic composition of the media used in both cases, Conti and Neher [28] calculated that under physiological conditions the directly measured conductance is 10 pS, in agreement with noise data.

Single K^+-channel records show kinetics that cannot be explained by a simple two-state open-closed model. Although the channel presents a single open conductance state, once it opens it shows short interruptions which are indicative that the open channel is in fast equilibrium with a closed state. The long time periods between bursts can be interpreted as a second closed state [28]. Kinetically, it can be represented by the sequential reaction scheme:

$$C_2 \underset{k_{-2}}{\overset{k_2}{\rightleftharpoons}} C_1 \underset{k_{-1}}{\overset{k_1}{\rightleftharpoons}} O \qquad \text{(R-1)}$$

where C_2, C_1, and O represent two closed states and a single open state, respecitively. If k_2 is small, then when the channel undergoes a transition

$$C_1 \xrightarrow{k_{-2}} C_2$$

it would be "locked" in that state. This is a minimal model, and the number of closed states may be larger than two. Conti and Neher have argued that a Hodgkin-Huxley type mechanism [69] does not give a fit to the single channel data.

For the K^+ channel of the node of Ranvier, a value of about 4 pS is obtained [15]. This value is lower than the 10 pS found in squid axons, and this is probably due to the difference in media composition. A correction of the squid K^+ channel conductance for the ionic composition of the frog node system, using the constant field equation, yields a value of about 4 pS, in good agreement with the measured values for the frog node K^+ channel. So far, the smallest conductance for the

delayed rectifier is that given by Reuter and Stevens [121] for the K^+ channel of snail neurons which, as we will see below, has a different and novel ion selectivity sequence. Interestingly, Neumcke et al. [113] found that K^+ channel conductances in the nodal membrane of myelinated and sensory nerves are different by a factor of 1.7 and that this indicates the presence of two different types of K^+ channels in these fibers.

Selectivity

The selectivity sequence for the nodal and squid axon delayed rectifiers is essentially the same, and only Tl^+, K^+, NH_4^+ and Rb^+ have measurable permeabilities in these channels [19, 20, 64, 65]. Moreover, both Cs^+ and Na^+ strongly block the K^+ channel (3, 19, 47). Both Bezanilla and Armstrong [19] and Hille [64] have postulated the existence of a localized "selectivity filter" inside the K^+ channel with a structure shown in Fig. 1. The selectivity filter is viewed in this model as the narrow part of the channel able to partially or totally dehydrate and closely interact with the permeant ion. The minimum pore diameter, arbitrarily defined by adjusting the size of a pentagon formed by five oxygen atoms, is 0.3–0.33 nm [65]. Thus, all ions larger than NH_4^+ (diam = 0.3 nm) are impermeant through the K^+ channel because of size considerations. The NH_4^+ ion itself permeates much more easily ($P_{NH_4^+}/P_{K^+} = 0.2$) than would be expected from its steric hindrance in such a model [20, 64]. Hille [65] therefore proposed that NH_4^+ makes hydrogen bonds with the K^+ channel and in doing so shortens the N–O center-to-center distance to 0.28 nm. Na^+ and Li^+, although smaller than K^+, cannot pass through the K^+ channel because oxygens forming part of the selectivity filter of the pore cannot approach closely enough to replace the waters of hydration. The model, therefore, works by exclusion of the impermeant ion rather than by selective binding of the more permeant ones. As pointed out by Armstrong [9], the model actually predicts *too much* selectivity, but this problem can be reduced by allowing some deformability of the pore walls (i.e., by permitting more interaction of Na^+ with the channel).

From reversal potential measurements, Reuter and Stevens [121] found for the delayed rectifier of snail neurons the following selectivity sequence: Tl^+ (1.3) > K^+(1) > Rb^+ (0.74) > Cs^+ (0.18) > NH_4^+ (0.15) > Li^+ (0.09) > Na^+ (0.07). Clearly this potassium channel is less selective to K^+ than either the nodal or the squid axon delayed rectifier, but what makes this selectivity sequence interesting

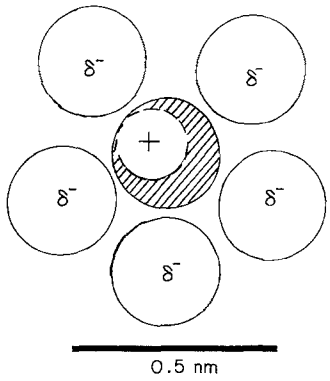

Fig. 1. Selectivity filter of delayed rectifier K^+ channel. A cross-section of the selectivity filter of the delayed rectifier, as modelled by Hille [64] is shown. The main features include five oxygen atoms shown with partial negative charge surrounding a space into which a dehydrated K^+ ion (shaded circle) fits. Also shown (unshaded circle inside shaded circle) is the size of a dehydrated Na^+ ion

is the relative positions of Li^+ and Na^+. This type of selectivity sequence is not a simple function of ionic radius nor does it conform to any of the eleven selectivity sequences given by Eisenman [42, 76].

In order to explain this experimental result, Reuter and Stevens [121] developed a new selectivity theory assuming that a single rate-limiting energy barrier controls ion transport through the channel. In it, the permeability ratio is given by:

$$Py/P_K = \exp\left[-(By - B_{K+})\, RT\right] \tag{1}$$

where By and B_K are the barrier energies for the ionic species Y and K^+, respectively. Furthermore, assuming only electrostatic interactions between the ion and its surroundings, the dependence of the barrier on reciprocal ion radius (X) can be explicitly expressed as a power series

$$B(X) = B(X_{K^+}) + a_1(X - X_{K^+}) + a_2(X - X_{K^+})^2 + a_3(X - X_{K^+})^3 \tag{2}$$

expanded about the reciprocal radius of the "reference" potassium ion (X_K). The number of terms in the series needed to be retained depends on how selective the channel is. For poorly selective channels, only the first two terms are required to describe the selectivity barriers, but for more selective ones, the quadratic and cubic terms need to be retained. The selectivity sequence of the snail delayed rectifier is obtained by retaining the first four terms of Eq. (2) and choosing the appropriate values for the coefficients a_1, a_2 and a_3. Furthermore, by using the Born [21] treatment for the free energy of a charged metal sphere in a dielectric

medium, Reuter and Stevens [121] could relate the coefficients of Eq. (2) with physical characteristics of the channel. For example, a_1 is related to the fixed dipole density at the surface of the reference ion as well as to the characteristics of the water structure in the channel compared with those in solution. Thus, the smaller the pore radius, the larger the coefficient a_1; a second way of raising a_1, argue Reuter and Stevens, is to make the channel more rigid, less able to accommodate multiple conformations in response to occupancy by ions of different sizes. This theoretical approach is still in its infancy, but because it endeavors to relate channel selectivity to channel architecture, it may provide a fruitful approach to future channel conduction studies.

Ion Blocking

As stated above, Cs^+, Na^+ or Li^+, when added to the internal medium, can block outward delayed K^+ currents. If an ion can block, it is because to some extent it can enter the channel but cannot pass through the selectivity filter. Cs^+ is the most powerful blocker of the three monovalent cations mentioned above, the sequence being $Cs^+ > Na^+ > Li^+$ [45]. One characteristic of the block by monovalent cations is that it is voltage dependent; the normally linear instantaneous I–V relationship for the delayed rectifier is transformed by blocker into a highly nonlinear I–V. Furthermore, with Cs^+ or Na^+, the instantaneous I–V develops a negative conductance at large depolarizations [19]. External Cs^+ can block inward but not outward K^+ currents, and the reverse is true when Cs^+ is added internally. One way to explain voltage-dependent block is that proposed by Woodhull [136]. It is assumed that somewhere along the channel there exists a site, S, that can bind a blocker ion, B^+, according to the sequence

$$S + B^+ \underset{k_{-1}}{\overset{k_1}{\rightleftharpoons}} BS. \qquad \text{(R-2)}$$

This reaction is characterized by a voltage-dependent dissociation constant, $K_D(V)$

$$K_D(V) = \frac{k_{-1}}{k_1} = \frac{[S]\,[B^+]}{[BS]}. \qquad (3)$$

From the principle of detailed balance, we have

$$\frac{n_o}{n_B} = \frac{k_{-1}}{k_1\,[B^+]} \qquad (4)$$

where n_o is the number of conducting sites and n_B the number of blocked sites. Now, at steady state, the probability of finding an open channel $[P_o]$ is simply

$$P_o = \frac{n_o}{n_o + n_B} \qquad (5)$$

which combined with Eqs. (1) and (2) gives

$$P_o = \left[1 + \frac{[B^+]}{K_D(V)}\right]^{-1}. \qquad (6)$$

Furthermore, if S is located at a fractional distance, δ, down the electric field, S "senses" a fraction, δV, of the total applied potential, V. Therefore, $K_D(V)$ will be voltage dependent according to the relation

$$K_D(V) = K_D(0)\, e^{-z\delta FV/RT} \qquad (7)$$

where $K_D(0)$ is the dissociation constant at zero voltage, z is the valence of the blocking ion, and F, R and T have their usual meanings [31, 136]. With Eq. (7), Eq. (6) becomes

$$P_o = \left[1 + \frac{[B^+]}{K_D(V)}\, e^{z\delta FV/RT}\right]^{-1}. \qquad (8)$$

Thus, by measuring currents (or conductances) in the presence or absence of B^+ and at different concentrations of B^+, the parameters $K_D(V)$ and δ can be calculated. There are several characteristics of the Cs^+ block that this single-site model cannot predict, but these problems can be overcome if one uses multisite single-file models [66]. For example, Adelman and French [3] found that the Cs^+ blockade of the inward K^+ currents is more voltage-dependent and the slope of the dose-response curve steeper than expected for a reaction following a 1:1 stoichiometry (i.e., Scheme R-2). In fitting their results to Eq. (8), they found $z\delta = 1.3$[1] Inasmuch as $z > 1$, one is forced to conclude that the K^+ channel is able to accept more than one ion at the same time [66]. This is consistent with the notion that the delayed rectifier is a multi-ion channel in which, as first suggested by Hodgkin and Keynes [70], ions are constrained to move in single file (*see* below).

French and Wells [47] made the interesting observation that the Na^+ block of the delayed rectifier can be relieved when large (+160 mV) depolarizing potentials are applied across the membrane. In other words, the K^+ channels become permeable to Na^+ at high positive potentials. They also

[1] If more than one blocking ion can occupy the channel, Eq. (8) has no theoretical meaning. However, when an empirical fit of the data to Eq. (8) leads to $\delta > 1$, it may be concluded that multiple ion occupancy applies [66].

showed that the block by tetraethylammonium (*see* below) could not be relieved by potential. This effect can be qualitatively predicted from the model given for the selectivity filter of Fig. 1, where Na^+ is discriminated with respect to K^+ by energetic and not steric considerations: The "bad fit" of Na^+ leads to a higher electrostatic energy for Na^+ than for K^+ in the selectivity filter [8]. Therefore, one can imagine that there is an applied voltage, V_C, such that the work necessary to pass through the selectivity filter (ΔU_{Na^+}) is exactly balanced by the electric work of moving Na^+ to the blocking site (zFV_C). Thus,

$$\Delta U_{Na} + zFV_C = 0. \tag{9}$$

French and Wells [47] found that the relief of Na^+ blockade by voltage starts at about +160 mV. Introducing this value in Eq. (9), we obtain $\Delta U_{Na} =$ 15 kJ/mol. Assuming further that $\Delta U_{K^+} \simeq 0$ for K^+, we have[2] from Eq. (1)

$$\frac{P_{Na^+}}{P_{K^+}} = e^{\Delta U_{Na}/RT} = 0.003. \tag{10}$$

This value is in reasonable agreement with the $P_{Na}/P_K = 0.01$ determined by Hille [64].

Effects of TEA and Derivatives

The delayed rectifier is also blocked by tetraethylammonium (TEA) ions and their analogues. TEA only depresses K^+ current when injected inside the axon in the squid, but in myelinated fibers the K^+ conductance is diminished by addition of TEA to either side [7, 10]. The effect of these ions on the internal site has been extensively reviewed by Armstrong [8, 9] and can be summarized as follows:

a) Internal quaternary ammonium ions (QA) can block only open channels.

b) Blocking potency increases as the hydrocarbon chains are lengthened, as if the binding site contained a hydrophobic region.

c) For compounds larger than TEA (e.g., triethylpentylammonium ion), the blocking is not "instantaneous" as is the case for TEA, but takes time to develop, causing an apparent "inactivation" of the K^+ current. This rate of blocking is increased by increasing the concentration of QA.

d) The unblocking reaction can be speeded up if the external K^+ concentration is raised, as if a K^+ ion coming from the outside medium were able to "clear" a blocked channel by pushing the blocking ion towards the internal solution. This is usually termed a "knock-off" mechanism. These observations imply that the site is in the channel itself.

e) Triethylammonium ions can be trapped inside the closed channel if the gates are rapidly closed by large hyperpolarizing pulses.

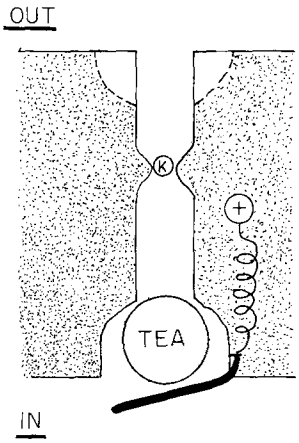

Fig. 2. Delayed rectifier model. The cartoon is drawn according to the main features discussed in the text: an internal TEA binding site within a mouth of about 1 nm diameter, a tunnel region, narrowing to a selectivity filter, and an external TEA binding site (dashed region) for the nodal channel. The "n^4 gate" is shown closing and trapping a TEA ion within the internal mouth

Armstrong [8, 9] concluded from these experiments that the potassium channel has a large intracellular mouth of about 0.8×0.8 nm that can accommodate TEA and other QA ions (Fig. 2). Hydrated K^+ and TEA^+ have the same diameter (0.8 nm) and can enter this wide part of the pore, but then the pore narrows and only K^+ can pass through if partially dehydrated (*see* above). Armstrong's experiments with QA ions suggested a specific location of the gating apparatus. The trapping of QA by hyperpolarization pulses indicates that the "n^4 gate" must be located towards the intracellular side (Fig. 2). Hille [65] found in myelinated nerves that the internal TEA blocking is well described by a one-site model [i.e., Scheme R-2, Eq. (8)] with $\delta = 0.2$ and $K_D = 5$ mM and that methylammonium blockage can be described with $\delta = 0.7$ and $K_D = 250$ mM. The most economical interpretation of these experiments is that small ions like methylammonium (0.3 nm) can go further into the delayed rectifier than TEA, implying that the selectivity filter is beyond the region where the wide mouth narrows.

The external receptor for TEA of the nodal delayed rectifier appears to be different from the

[2] U is taken as a single rate-limiting energy barrier to sodium transport through the potassium channel. The activation energy for aqueous K^+ conductance and that for channel conductance are essentially the same [44], implying that the nondiffusional barrier (i.e., ΔU_K) must be very low.

internal one. First, blockade of the channel by external application of TEA is voltage- and time-dependent. Second, the affinity of the site for TEA is higher than for the long hydrocarbon chain QA. This indicates that the external receptor lacks the hydrophobic moiety of the internal receptor.

More recently, two groups have restudied the blocking of K^+ channels by QA ions using TEA derivatives of different sizes [46, 132]. Their results can be interpreted in terms of the single site blocking proposed in Scheme (*R*-2) that can be translated in terms of channels closed, open, and blocked as

$$\ldots \text{Closed} \rightleftharpoons \text{Open} \underset{k_{-1}}{\overset{k_1[B^+]}{\rightleftharpoons}} \text{blocked}. \qquad \text{(R-3)}$$

Swenson [132] used a series of QA ions within which the N-substituents varied in length and polarity. He found first, and contrary to the expectation of Armstrong's model, that compounds with polar head groups as large as 1.1×1.2 nm were able to occlude the channel (e.g., octyltripropylammonium, C_8TP). Second, compounds containing hydrophilic constituents (e.g., octyltriethylethanolammonium, C_8TE_{toh}) are low-affinity blockers. For example, K_D's for C_8TP and C_8TE_{toh} are 28 and 1,100 mM, respectively. Third, the blocking site for all compounds appears to be located at $\delta \simeq 0.2$. French and Shoukimas [46] used QA ions of the type $(C_nH_{2n+1})_4N^+$, $n=1$–6. In agreement with Swenson's results, they found $\delta \simeq 0.2$ for all compounds with $n=2$–6, but $\delta = 0.4$ for $n=1$. We recall here that $\delta = 0.7$ for methylammonium in the nodal delayed rectifier [65]). They also found that blocking potency increased with QA size in a complicated way. These results together imply that a great deal of hydrophobic interaction is allowed in the first "antechamber" of the delayed rectifier and that the dimensions for the mouth of the pore, 1.0×1.2 nm, proposed by Swenson [132] are reasonable.

Divalent Cations also Block the Delayed Rectifier

Both squid axon and muscle delayed rectifier channels are blocked by Ba^{2+} ions [11, 39, 54]. The block by internal Ba^{2+} of the squid axon channel displays characteristics of unusual simplicity in this otherwise complicated channel. Ba^{2+} blocks with exceptionally high affinity, with a dissociation constant of 0.1 μM at zero voltage [39]. The dissociation constant varies exponentially with voltage [Eq. (7)], such that the binding site appears to be located at an electrical distance, δ, of 0.5–0.7, substantially farther into the channel than the sites for TEA ($\delta \sim 0.2$) or TMA ($\delta \sim 0.4$) discussed above. Because the block is so strong, the kinetics of entry and exit of Ba^{2+} can be resolved. Eaton and Brodwick [39] found that the exit rate is extremely slow; at -70 mV, a Ba^{2+} ion spends, on the average, 700 msec in the channel before dissociating. (Compare with a typical residence time for K^+ inside the channel of 0.1–1 μsec). A dissociation rate of this magnitude would correspond to a free energy barrier for exit of about 110 kJ/mol [39], much higher than the barriers involved in the movements of the conducting ions. Thus, there is apparently a site within the channel which can specifically interact with Ba^{2+} so that the ion experiences a deep energy minimum there.

In striking contrast to the cases of block by monovalent cations, Ba^{2+} block shows no characteristics of multiple ion interactions inside the channel – no anomalous voltage dependence or current-dependent behavior. Instead, Ba^{2+} and K^+ act in a simple competitive relationship; if the channel is occupied by K^+, then Ba^{2+} cannot enter, and vice versa [39]. In other words, the channel obeys a single-ion occupancy rule for Ba^{2+}. This makes the physical interpretation of the Ba^{2+} blocking phenomena much less equivocal than in the case of the multi-ion blockers [67].

We can ask how much energy would be required to transfer a Ba^{2+} ion from aqueous solution into the pore. Assuming a channel diameter of 0.5 nm, consistent with the sizes of the quaternary ammonium blockers, electrostatic calculations according to Levitt [89] or to Parsegian [119] lead to an image-force barrier for entry of Ba^{2+} of 80 kJ/mol or 190 kJ/mol, respectively. These numbers are quite uncertain, but Jordan [73] has given reasons to think that the true value for the image-force energy should lie between these two values. Thus, it would seem that the Ba^{2+} ion should be excluded from the channel simply on the basis of these energies, which are so large mainly because of the divalent nature of the ion.

Eaton and Brodwick [39] have performed an interesting thermodynamic analysis of Ba^{2+} block by studying the effect of temperature on the Ba^{2+} blocking kinetics. The entry rate of Ba^{2+} is extraordinarily temperature-dependent, with an activation enthalpy of 140 kJ/mol. An energy barrier of this magnitude is entirely consistent with the electrostatic calculations above. However, the entry rate is enhanced by an extremely favorable *entropy*, which lowers the total free energy barrier to a manageable 60 kJ/mol. After crossing this barrier, the Ba^{2+} ion falls 110 kJ/mol into a deep free energy

well of -50 kJ/mol, i.e., into a strong, specific binding site.

Why might Ba^{2+} act as such a strong blocker? It has been suggested [38, 11] that Ba^{2+} can interact with the same sites as does K^+, since the two ions have very similar unhydrated crystal diameters (0.270 and 0.267 nm, respectively). If we take seriously Hille's model of the selectivity filter (Fig. 1), in which an unhydrated K^+ ion fits precisely, we could imagine that the higher charge on Ba^{2+}, combined with its excellent size-match to K^+, would cause a tight binding of the divalent ion to the selectivity filter itself. In other words, Ba^{2+} may be acting as a classical "transition state analogue" for this channel. If this picture is valid, the position of the selectivity filter is uniquely determined at $\delta = 0.5$–0.7. These are speculative notions, but the idea that Ba^{2+} is largely dehydrated inside the channel is consistent with the large activation *entropy* of Ba^{2+} entry [34].

Unidirectional K^+ Fluxes

Ever since Hodgkin and Keynes [70] established the "anomalous" behavior of unidirectional K^+ fluxes in voltage-clamped squid axons, it has been understood that some sort of "single-file" or "long pore" model of diffusion through the delayed rectifier must be envisioned. The original work showed that at a constant voltage, unidirectional K^+ *efflux* is inhibited by K^+ in the *external* medium. Furthermore, it was found that the flux ratio exponent, a measurement of the voltage-dependence of the ratio of inward and outward fluxes, is greater than unity. Since Ussing [133] had previously shown on very general grounds that this parameter must always be unity for independent ion movement, Hodgkin and Keynes realized that several K^+ ions must be able to interact within the delayed rectifier. Recently, Begenisich and De Weer [14] made careful measurements in axon of the flux ratio exponent of the delayed rectifier channel under a wide range of conditions. They found that as K^+ concentration is elevated, the flux ratio exponent increases monotonically from a low value of 1.5 to a high value of 3.3. In addition, they showed that at a fixed K^+ concentration, the exponent increases with increasing hyperpolarization. These findings were taken to imply that at least two, and probably three, K^+ ions can be simultaneously loaded into the K^+ channel, and that this multiple-ion occupancy is favored at high K^+, as expected, and at hyperpolarized potentials, as if the K^+ binding sites are located towards the cytoplasmic side of the channel.

Conclusion – A Fanciful Picture of the Delayed Rectifier

Following Armstrong [8, 9] we envision the delayed rectifier as having a wide mouth towards the interior of the cell, large enough to be able to accommodate TEA ($r \simeq 0.8$ nm) and triethanol-containing QA ions (~ 1.0 nm; Fig. 2). Inasmuch as these ions induce a voltage-dependent block, they must interact with sites located inside the channel. Furthermore, the nodal delayed rectifier contains an external QA ion receptor with properties different from the inner one [10]. The interaction with this site is voltage- and time-independent, and TEA is more effective than some hydrophobic QA ions. These observations suggest the existence of two separate TEA sites in the nodal channel. The TEA experiments also suggest that the channel "gate" is a localized structure lying between the cytoplasm and the inner QA ion receptor site.

Beyond the internal TEA site, the wide mouth narrows to a diameter large enough to accommodate TMA (~ 0.5 nm), at about 40% of the voltage drop [46], and methylammonium [65], with a size of $0.35 \times 0.37 \times 0.41$ nm, at 70% of the voltage drop. Further narrowing of the channel, to about 3 Å, allows for perfect K^+ fitting. Ions larger than K^+, like Cs^+, fail to permeate because of size (0.338 nm diameter). Smaller ions like Na^+ (0.190 nm diameter) do not go through because of energy considerations.

There are numerous arguments demonstrating that the delayed rectifier is a multi-ion single-file pore [66, 67]. The key indications of multiple ion occupancy are the violation of the Ussing flux ratio relation [14], and an effective valence greater than unity for the Cs^+ blocking reaction [3]. The single filing and multiple occupancy probably take place in the region between the large mouth and the selectivity filter, and between the selectivity filter and the external solution. Single-file restriction may arise both from ion-ion repulsion as well as from steric constraints imposed by the pore's wall. It is possible then, as pointed out by Hille and Schwarz [67], that "the mechanical pore diameter could be larger than two K^+-ion diameters throughout much of the channel."

Inward Rectifier

Channel Conductance Characteristics

Since the late 1940's [74], it has been known that the resting K^+ permeability shows inwardly-rectifying characteristics. Katz observed that in isotonic K_2SO_4 the conductance of the frog muscle mem-

brane for outward current was much less than the conductance for inward current. This property is known as inward or anomalous rectification and is shared by cell membranes of skeletal muscle [68, 74, 131], egg [57], and neurons [17]. The inward rectifier has the eccentric property that its conductance appears not to be a function of the membrane potential *per se* (as in the case of the delayed rectifier), but rather of the electrical *driving force* for K^+, V-E_K. Its conductance is high for voltages more negative than E_K (inward current), and low for voltages positive to E_K (outward current), regardless of the absolute value of E_K. Recently it has been shown in frog muscle that the channel is controlled by membrane potential and external K^+ concentration [88] as well. Single-channel measurements on this system have only just begun, and our view of this channel is still quite primitive.

Noise measurements in intracellularly perfused tunicate eggs gave a channel conductance for the inward rectifier of 5.5 and 7 pS in 50 and 100 mM external K^+, respectively [114]. Direct recordings of the single channel currents of the inward rectifier of tunicate eggs confirmed this value of channel conductance in 50 mM K^+ [115].

In cultured rat myotubes, single K^+ channel currents of the inward rectifier were resolved using the patch-recording method [116]. In order to record single channel currents, *all* the channels in the membrane patch were activated by filling the patch electrode with isotonic KCl (150 mM).[3] Current fluctuations were elicited by introducing low concentrations of Ba^{2+}, a "slow" blocker of the inward rectifier ([128]; *see* Ba^{2+} block of the delayed rectifier). The unitary currents detected as current fluctuations due to the blocking and unblocking of channels by Ba^{2+} is 10 pS. Similar fluctuations induced by Cs^+ in the frog muscle inward rectifier [125] also give 10 pS conductance. For the egg inward rectifier, the channel conductance is apparently proportional to the square root of the external K^+ concentration [57, 114]. The significance of this result is not clear.

Selectivity and Block

The inward rectifier selectivity sequence of starfish egg cells parallels that of the delayed rectifier; i.e., Tl^+ (1.5) > K^+ (1) > Rb^+ (0.3–0.4) > NH_4^+ (0.03–0.04) ≫ Na^+ > Cs^+ [57]. Thus, the inward rectifier is able to select K^+ over Rb^+ and NH_4^+ three- to fourfold more efficiently than the delayed rectifier. For the inward rectifier in frog muscle, P_{Tl^+}/P_{K^+} is 1.1, and the permeability of the other group *Ia* cations is immeasurably low [50, 130].

Inward rectification in both egg cell and muscle membranes is blocked by externally applied Cs^+, Na^+, and Li^+ [51, 56, 125]. In all cases the block is voltage dependent, as with the squid axon delayed rectifier, but some notable differences are apparent in the inward rectifier. In the starfish egg, Cs^+ blocks over 10-fold more strongly than in the squid axon, and the time-dependence of the block can be resolved [56]. In this respect, Cs^+ block of the inward rectifier resembles QA block of the delayed rectifier. The block of the egg inward rectifier [114] by Na^+ is relieved at high negative potentials, as though at very high driving force, Na^+ is able to "punch through" the selectivity filter, as in the delayed rectifier (*see* above). A complication in the egg system is that at low potentials, Na^+ appears actually to increase K^+ current, for reasons which are entirely unknown [114], but this effect is not present in muscle [129]. The exquisite selectivity of the inward rectifier of muscle is also illustrated by the fact that even Rb^+ blocks this system, with relief of block at high potentials [130].

The voltage dependence of the blocking by all the above ions is anomalously strong for both the egg and muscle inward rectifiers, with values for the effective electrical distance, δ, [Eq. (8)] in the range 1.3–1.4. This characteristic is a strong indication that the inward rectifier, like the delayed rectifier, is a multi-ion channel [66, 67].

Divalent cations, Ba^{2+} and Sr^{2+}, added externally, are also able to promote time- and voltage-dependent block in this channel [55, 128]. As in the delayed rectifier, the electrical distance δ for Ba^{2+} block of the muscle inward rectifier is *not* anomalously high, but has a value of 0.7, about half of that of the monovalent blockers. This result tempts one to speculate that only a *single* divalent blocker may enter this channel, because the charge-charge repulsion would be too great to allow two such ions to enter, in contrast to the situation for monovalent blockers.

Externally applied TEA (80 mM) blocks inward rectification in a voltage *independent* way [131]. Thus, the external TEA receptor of this channel displays a low affinity for the ion, and acts as though it is entirely outside of the applied electric field.

Finally, the multiple ion occupancy of the inward rectifier of frog muscle has been demonstrated by measurements of unidirectional K^+ fluxes through this pathway [127]. Here, external

[3] Under these experimental conditions, V_K at the patch is ~0 mV and, therefore, if the patch electrode is held at the bath potential, V–V_K at the membrane patch is −70 to −80 mV. At this potential the inward rectifier channels in the patch are expected to be activated [4].

K^+ was varied in fibers "clamped" at zero voltage with high Cl^-, under conditions of inactivation of the delayed rectifier. The flux ratio exponent was found to increase up to a value of 2.0 as K^+ was increased up to 300 mM. At least 2 K^+ ions, therefore, are able to occupy this channel simultaneously. A higher flux ratio of 3 was found in the delayed rectifier of squid axon [14] under similar ionic conditions.

Conclusions

The similarities in unitary conductance, ionic selectivity, unidirectional fluxes, and blocking behavior between the inward and delayed rectifiers are striking enough to lead one to postulate a basic architectural blueprint common to these two K^+ channels. Each channel contains an external (wide mouth?) TEA receptor. Towards the cell interior, the channel diameter is large enough to accommodate Cs^+ and long enough to allow simultaneous occupancy by at least two, and possibly three, ions. Farther into the channel is found a selectivity filter finely tuned for K^+ selection.

As similar as these two channels are, we cannot view them as identical pore-structures differing only in their gating mechanisms. The inward rectifier discriminates more closely than the delayed rectifier among alkalai metal cations, and the monovalent blocking ions bind more strongly to the inward rectifier. These two facts indicate that although the types of liganding interactions involved in diffusion through these channels are similar, the magnitudes of the energy maxima and minima experienced by a permeating ion are different. In terms of Hille's view of the K^+ channel selectivity filter (Fig. 1), and in terms of the "polynomial" selectivity theory of Reuter and Stevens [Eq. (2)], we would say that the filter of the inward rectifier is a more rigid structure than that of the delayed rectifier, less able to adjust its dimensions to allow favorable liganding even with as close a K^+ analogue as Rb^+. Tl^+ ion, of course, would be able to permeate both channels well, since its "soft" high-level orbitals allow it to adjust its own structure to that of the channel filter.

Maxi K^+ Channels

Sarcoplasmic Reticulum K^+ Channel

The first of this class of channels to be recognized as unusually large and selective is the K^+ channel from mammalian sarcoplasmic reticulum (SR) [34, 101]. The channels are studied by inserting them into planar phospholipid bilayers by fusion of SR membrane vesicles [107]. By varying the degree of fusion, it is possible to obtain bilayers containing as many as 10^4 channels or as few as a single channel [79]. For our purposes here, we are concerned only with the open-state ion conduction properties of this channel.

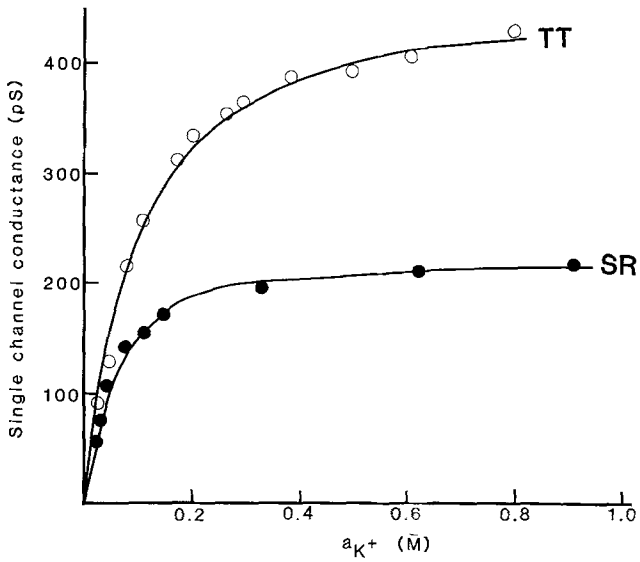

Fig. 3. Conductance-activity relations for maxi K^+ channels. Single channel conductance γ for SR or TT K^+ channels are shown as a function of K^+ activity, a_K. Determinations were made at 20 °C, in symmetrical KCl solutions. Solid curves are drawn according to Eq. (13). Parameters are: for SR channel, $K_D = 50$ mM, $\gamma_{max} = 230$ pS; for TT channel, $K_D = 140$ mM, $\gamma_{max} = 500$ pS. SR data taken from Ref. [34] and from C. Miller and M. Barroll (*unpublished*). TT data taken from C. Vergara and R. Latorre (*unpublished*)

The SR K^+ channel shows substantial selectivity among monovalent cations, the only class of ions permeant to this channel [34]. For instance, the channel conductance is threefold and 25-fold higher for K^+ than for Na^+ and Li^+, respectively. The channel conductance follows a "Michaelis-Menten" law for all the conducting cations; as cation concentration increases, the single channel conductance rises at low concentrations and reaches a saturation value at high concentration (*see* Fig. 3). Several points about these saturation curves are noteworthy. The maximum conductance for K^+ is large (230 pS). In addition, the apparent dissociation constants are quite low for this channel, 54, 34, and 19 mM for K^+, Na^+, and Li^+, respectively.

Under symmetrical salt conditions, no conductance for Cs^+ can be detected; indeed, Cs^+ in the 10 mM range blocks the K^+ current through the channel [31, 34]. A variety of quaternary amines also block this channel [33]; TEA is a rather weak

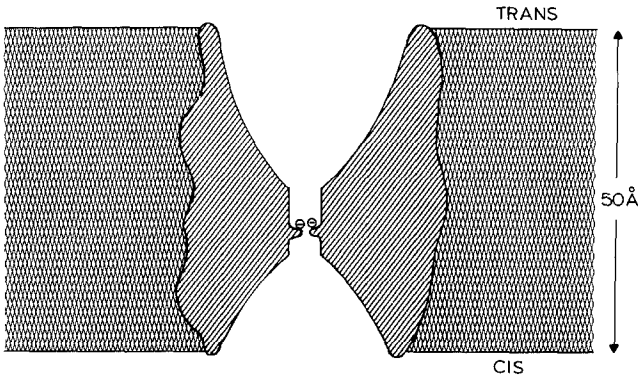

Fig. 4. SR K^+ channel model. Cartoon of SR K^+ channel is drawn to scale, according to size measurements based on organic cation conduction, block, and on streaming potentials. A short tunnel region of 1 nm in length and 0.7 nm in width is shown connected to the external solutions via mouths much wider than 1 nm. A selectivity filter of 0.4 nm width is placed 0.6 nm into the tunnel from the *trans* side of the membrane. Two titratable charges are placed at the selectivity constriction. Figure taken from ref. [104]

blocker ($K_i = 86$ mM at zero voltage), while bis-quaternary analogues of decamethonium block the SR K^+ channel at μM concentrations [32, 102]. These divalent cations fail to block the delayed rectifier of squid axons (M. White and F. Bezanilla, *personal communication*). The blocking by all of these compounds is purely voltage dependent and competitive with K^+ in a way which suggests that the compounds literally enter and plug up the K^+ conduction pathway [33].

The point we wish to make here is that, in contrast with both the delayed and inward rectifiers, the conduction mechanism of this channel may be understood in terms of a single-ion model [85, 87], in which the channel can be occupied by at most one ion at a time [34, 102]. Application of such a simple model enables us to draw conclusions about the structure of the channel more easily than would be the case if a more complicated, multi-ion model applied, as with the inward and delayed rectifiers. For example, the voltage dependence of blocking can, using a single-ion model, be translated into a real "electrical distance" of the blocking site, since in such a case there are by definition no current-dependent "knock-on" phenomena inolved [102]. By probing this channel with a variety of blockers and conducting "organic cations," and by measuring streaming potentials [103], it has been possible to derive a rough picture of this channel's conduction pathway (*see* Fig. 4) as containing very wide mouths (>1 nm in diameter) on one or both sides, in series with a "short tunnel" of about 0.7 nm in diameter and 1 nm length in which the applied voltage drops, and a critical constriction of 0.4–0.5 nm diameter located 0.6–0.7 nm in from one end of the tunnel. It is presumably at this constriction that the bulk of ion selectivity takes place. The work leading to this picture has been reviewed elsewhere [104].

A Digression on Hemocyanin

Hemocyanin is the major oxygen-carrying protein in the hemolymph of marine invertebrates such as crustaceans and mollusks. Unaccountably, it forms high-conductance channels in lipid bilayers [5, 82, 99]. The channel is selective to cations but does not completely exclude Cl^- [22, 24]. Because of the type of ion selectivity presented by the hemocyanin channel, it does not fall into the "maxi K^+ channel" category (Table). However, several of its conduction characteristics are similar enough to these that it is worthwhile mentioning them here. As in the SR channel, hemocyanin behaves as though no more than one ion is allowed inside the channel at a given time. Furthermore, given the single ion occupancy condition, a three-energy-barrier model, in which the entrance and exit barriers are out of the electric field, with the barrier for ion transport inside the field, can explain the nonlinearity of the *I–V* curves, as well as ion competition and zero-current potentials [22]. The ion conduction is blocked by tris and TMA ions in a voltage-dependent manner, indicating that the hemocyanin channel, as in the case of other K^+ channels, has wide mouths. These wide mouths are apparently located at least a Debye length (10 Å) away from the membrane surface (since the channel's mouths do not sense the surface potential of the lipid membrane [22]). As with the SR K^+ channel, the critical single-filing region of the channel was sized by measurement of streaming potentials [23]. These were found to be very low, and the conclusion was reached that at most two water molecules and a K^+ ion are constrained to move in single file through the channel. This, in turn, places an upper limit of 0.6 nm on the length of any region inside the channel narrow enough to forbid K^+ and water to pass one another. Thus, the electrical characterization of the channel leads to a picture of a "short tunnel" of perhaps 0.5–0.6 nm in diameter, in series with wider mouths on either end.

The recent structural work of McIntosh et al. [94] is consistent with such a model. In liposome membranes, the protein forms a structure visible in the electron microscope. This structure, which is seen only in channel-forming hemocyanins, is a cylinder of about 10 nm in length; when viewed along the cylindrical axis, accumulation of stain occurs in a pit of approximately 2 nm diameter,

a size consistent with the wide mouths postulated from the electrical work.

Maxi Ca^{2+}-Dependent K^+ Channels

In many types of cells, an increase in cytoplasmic Ca^{2+} concentration triggers a K^+ conductance. This effect was first discovered by Gardos in erythrocytes [49]; later, Meech [95] and Krnjevic and Lisiewicz [77] found a similar phenomenon in neurons. As pointed out by Meech [96, 97], the Ca^{2+} influx entering the nerve cell during a brief depolarizing pulse is able to activate this K^+ conductance, usually termed $G_{K(Ca)}$, which gives rise to a long lasting hyperpolarization. Ca^{2+}-dependent K^+ conductance is ubiquitous and plays an important role in regulating repetitive activity in both invertebrate and vertebrate neurons (for a review, *see* Ref. 96).

Hermann and Gorman [62] have studied the selectivity of the Ca^{2+} "receptor" of this channel as well as its conduction characteristics, using a classical voltage-clamp approach in *Aplysia* neurons. Ca^{2+} is the most effective activator of the conductance, followed by Cd^{2+}, Hg^{2+}, and Sr^{2+}. Ba^{2+} ion was found to block the Ca^{2+}-activated conductance. The alkali metal ion selectivity of the conductance is reminiscent of that of the delayed rectifier: K^+ (1) = Tl^+ (1) > Rb^+ (0.7) > NH_4^+ (0.1) ≫ Na^+, Li^+ [52]. Since the Ca^{2+}-activated K^+ conductance of *Aplysia* has not yet been observed on the single-channel level, we do not know if this falls in the maxi-K^+ channel category. However, we think it likely that this will be the case, since recently single Ca^{2+}-dependent K^+ channels have been detected in a wide variety of other cells (Table), and nearly all of them have been found to be unusually large and selective.

Characteristics of Single Ca^{2+}-Dependent K^+ Channels

Of the seven high-conductance Ca^{2+}-dependent channels which have so far been described on the single-channel level, we have at present detailed information about conduction and selectivity for only one of them, the Ca^{2+}-dependent K^+ channel of rabbit skeletal muscle plasma membrane [84]. This channel has been studied in planar bilayers after incorporation of plasma membrane vesicles under conditions similar to those used for SR K^+ channels [106]. The gross properties of the other Ca^{2+}-dependent channels are in many aspects similar to those of this transverse tubule (TT) Ca^{2+}-dependent K^+ channel from rabbit muscle; we are, therefore, confident that the molecular architecture

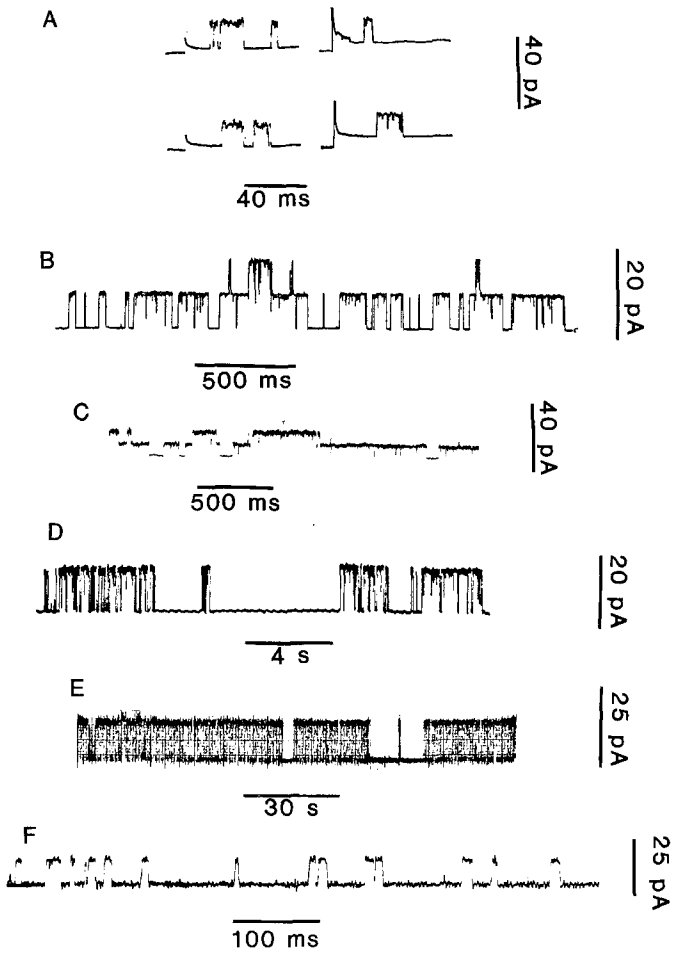

Fig. 5. Maxi Ca^{2+}-dependent K^+ channel activity in different preparations. (*A*): Unitary currents in isolated patches of chromaffin cell membranes. Top left record was obtained by applying a 75-mV depolarizing pulse from a holding potential of 0 mV. External medium contains isotonic (143 mM K^+) Ringer and 1 Ca^{2+}-11 EGTA buffer, pH 7.3. Bottom left record was obtained at the same applied potential but in an inside-out patch. Top right record: the pipette containing isotonic KCl was applied to a cell bathed in normal Ringer. The patch holding potential is about −60 mV. The record was obtained with a 100-mV depolarizing pulse. Bottom right record was obtained by applying a 104-mV depolarizing pulse to an inside-out patch (from Ref. 92). (*B*): Single-channel currents recorded from a patch of a membrane in an intact myotube at a potential of +50 mV at the patch. The cell was bathed in normal Ringer. Assumed external $[Ca^{2+}]$ 5×10^{-7} M (from Ref. 117). (*C*): Single-channel activity in sympathetic ganglia cells when the membrane patch was depolarized by 150 mV. Internal $[Ca^{2+}]$ unknown (from Ref. 2). (*D*): Single-channel activity in clonal anterior pituitary cells. Membrane patch depolarized 55 ml from rest. Resting potential was ~ −50 mV. Isotonic K^+ Ringer containing 5×10^{-7} M Ca^{2+} was used as the bath solution, and the pipette was filled with Ca^{2+}-free Ringer (from Ref. 135). (*E, F*): Single-channel currents of muscle transverse tubule membrane Ca^{2+}-activated K^+ channels in a planar lipid bilayer. The solutions were symmetrical 0.1 M KCl and contained 1.5×10^{-5} M Ca^{2+}. The first record (*E*) was obtained by applying a pulse of +70 mV. (The side where membrane preparation is added is defined as positive.) *F* was obtained by applying a potential of +50 mV (from C. Vergara and R. Latorre, *unpublished*). Note similarities in kinetics as well as conductances between different records

of all the channels in this group (at least for the ion conduction pathway) will prove to be similar. In Fig. 5, tracings of unitary fluctuations are shown for a variety of those Ca^{2+}-activated channels. A number of properties are held in common by these channels. *First*, for all channels tested, the conductance of the channel in symmetrical solutions of 0.15 M K^+ is very high, >180 pS (*see* Table). *Second*, both the TT-channel [84] and that of vertebrate sympathetic neurones [2] are highly sensitive to external TEA, with blocking constants in the range of 0.1–1 mM. The Ca^{2+}-dependent K^+ channel from pituitary cells [135] is insensitive to external TEA but is blocked by high (~20 mM) concentrations of TEA added to the cytoplasmic side. The TT channel is also blocked by "internal" TEA. Channel conductance is halved when the TEA concentration in the *cis* side is ~10 mM (C. Vergara and R. Latorre, *in preparation*). In this regard, therefore, the TT channel presents internal and external receptors for TEA like the nodal delayed rectifier. *Third*, all the channels in this group are perfect K^+-electrodes. In both rat axolemma and cultured rat muscle channels [78, 100, 117], it appears that the sodium permeability is unmeasurably low. For the TT channel, a K^+/Na^+ permeability ratio of 7 was reported [84], but recent results indicate that this value is much higher; no reversal potential can be found under K^+/Na^+ bionic conditions, as the single channel I–V curve approaches the V axis asymptotically (C. Vergara and R. Latorre, *in preparation*). The same result holds for Rb^+ and Cs^+. Thus, like the inward rectifier, the TT K^+ channel is highly selective for alkali metal ions. But its conductance is about 50-fold larger than that of the inward rectifier. *Fourth* $G_{K(Ca)}$ changes e-fold every 11, 12.5 and 28 mV for the vertebrate sympathetic neurons, the TT, and the pituitary cell Ca^{2+}-dependent channels, respectively [2, 84, 135]. The voltage dependence of the $G_{K(Ca)}$ of the rat cell culture channel is identical to that obtained for the Ca^{2+}-dependent TT channels [100]. *Fifth*, there is a striking similarity between the opening and closing kinetics of the channels in those cases that have been studied in some detail [84]. These show at least two closed states and one open state. The curve of the open state probability P_o of the channel as a function of membrane potential appears to shift along the voltage axis with changes in the internal Ca^{2+} concentration. The shift in P_o with a 10-fold change in Ca^{2+} concentration is ~65 mV. This is consistent with the hypothesis that 2–3 Ca^{2+} are required to open one Ca^{2+}-dependent K^+ channel [8, 100, 135]. However, the Ca^{2+} sensitivity varies from channel to channel. For example, P_o is 0.5 at −20 mV for 1 μM Ca^{2+} for the pituitary cell channel [135] and 8 μM for the rat muscle channel [100]. A $[Ca^{2+}]$ of 1 mM is required to obtain the same P_o at the same potential for the TT channel [84].

Finally, it appears that the TT K^+ channel operates by a simple, single-ion mechanism as with the SR K^+ channel, and in contrast to the delayed and inward rectifiers (e.g., Fig. 3).

Can We Reconcile Large Channel Conductances with a High Selectivity?

The Main Problem: Diffusion Limitation

The remainder of the review will deal with the strange behavior of the maxi K^+ channels, the combination of high conductance with high ionic selectivity. As mentioned above, inspection of the Table shows how anomalous this behavior is, viewed in the context of other ion channels. In addition, from an intuitive point of view, these channels seem bizarre. How can they select for K^+ ions so exquisitely without slowing them down?

Are we perhaps not making too much of this anomaly? Shouldn't we merely say that intuitive notions of conductance and selectivity are not likely to be correct all the time, and that we only have identified a class of channels that violates intuition? In fact, the problem is more serious than this, because the high conductances of these channels appear at first glance to surpass the upper limits imposed by the rates at which ions can diffuse up to the channel from aqueous solution, or through the channel by unrestricted diffusion.

Radius of Equivalent Conductivity Pore

Consider the simplest model of the channel as an electrolyte-filled cylinder of the same conductivity as the aqueous medium. Then, the channel conductance, γ, is given by:

$$\gamma = \Lambda \pi r^2 / l \tag{11}$$

where Λ is the single ion conductivity, r is the pore radius, and l the length of the pore. Assuming that l is 5 nm, then a channel of 130 pS in 0.1 M K^+ (the SR channel) would have a radius of about 0.4 nm, much too large to allow intercationic selectivity, single-ion behavior, saturation, or single-site competitive blocking. The problem is not that this unrealistic calculation disagrees with a reasonable channel radius, but rather that it is hard to imagine

a realistic transport mechanism that would be *faster* than free, homogeneous diffusion and still give tight ionic selectivity.

Empirical Evidence: Gramicidin A Channel

In an elegant analysis of conduction in gramicidin A, Andersen and Procopio [6] have observed an upper limit for current through this channel and have proposed that this is due to diffusion-limited access to the channel of the ions in solution. In other words, as voltage is increased to very high values, the current reaches a plateau level because the rate-limiting step for transport through the channel becomes diffusion up to the channel's mouth. For gramicidin, with 0.1 M Rb^+, this upper limit is only 3.2 pA. This is disturbing because we know that at a similar concentration of K^+, the TT and SR channels show linear current-voltage relations up to at least 125 mV, with conductances of 212 and 130 pS, respectively; that is, there is not even a hint of saturation of current even at 26 pA for the TT channel, eightfold higher than the limiting current through the much less selective gramicidin A channel. Again, the currents through these maxi K^+ channels are "too high."

Calculation of Convergence Conductance

Several authors have pointed out that if the permeability for a given ion is high, the overall transport will be ultimately limited by the rate at which ions from the solution arrive at the channel entrance [6, 58, 86]. The problem of diffusion-limited transport through channels was treated in detail by Läuger [86] who modeled the transport process as a three-compartment system, composed of a channel with an inherent conductance flanked on each end by aqueous regions with a "convergence conductance." This convergence conductance represents the diffusion of ions up to or away from the channel, and it was assumed that the Nernst-Planck treatment of homogeneous, independent electrodiffusion provides a valid description of ion movement in this aqueous region. It could then be shown that a cation-selective channel separating symmetrical solutions of 1:1 electrolyte will display a convergence conductance A_c (at ion concentration c low enough for the conductance to depend linearly on ion concentration) given by:

$$A_c = \frac{2\pi F^2 D}{RT} r_o c \qquad (12)$$

where D is the aqueous diffusion coefficient of the ion. In Eq. (12) the crucial parameter, r_o, is the "capture radius" of the channel, and it defines the area available for a freely diffusing ion to "collide with" the entry of the channel. As such, it does not represent the equivalent radius of the physical opening of the channel but rather the difference between this radius and that of the diffusing ion[4] [6].

The convergence conductance places an absolute upper limit of the zero-voltage conductance of any channel, but its precise value requires a knowledge of the structure of the channel. Fortunately, the structure of the gram A channel is known [75], and it is possible to test the validity of the above treatment. For Rb^+ entering the gram A channel, the capture radius is about 0.05 nm [6], and application of Eq. (12) then predicts that the channel can never have a zero-voltage conductance greater than about 1 nS/M. Gram A, in fact, displays conductances of 50–100 pS/M, well below this limit. This calculation uses a 0.2 nm radius for the channel opening, and it is unlikely that the size of the selectivity region of the maxi K^+ channels can be much larger than this, or they would not display high ionic selectivity. Using the information of Fig. 3, which shows the relation between zero-voltage conductance and ion activity for the SR channel and the TT channel, we find that the linear range zero-voltage conductances are 5 nS/M and 3 nS/M for the SR and TT channels, respectively. These are over 50-fold higher than the values for gram A, and well beyond the diffusion limit for the nonselective gram A channel. Once again, the anomalous K^+ channels are "too large."

The point of presenting these three examples is not to suggest that the maxi K^+ channel conductances are impossibly high, but rather to bring the problem of these high conductances into quantitative focus. Stated again, the problem is that simple models using pore sizes small enough to give substantial ionic selectivity predict that the channel will not be able to pass the large currents at high voltages or to display the large conductances at low voltages that are actually observed. We now consider several possible escapes from this apparent contradiction.

First, it is necessary to realize that for both the SR and TT channels, there are really *two* rate processes which must be clearly distinguished. These are both channels in which the conductance saturates as concentration is increased. Both the SR channel and TT channels saturate in a simple

[4] Somewhat larger values (1.5- to 3-fold) for r_o are possible if an ion hits the membrane and then diffuses to the channel mouth along the membrane surface [1].

"Michaelis-Menten" fashion (Fig. 3), as though only a single ion can occupy the channel at a time. Thus the channel conductance is described by:

$$\gamma = \frac{\gamma_{max} \cdot a_K/K_d}{1 + a_K/K_d}. \quad (13)$$

The initial slope of the saturation curve, γ_{max}/K_d, represents the second-order rate process of an ion *entering* the channel (or, more precisely, of an ion going from aqueous solution to the highest transition state of the free energy profile of the channel); the maximum conductance, γ_{max}, represents the first-order rate process of an ion *leaving* the channel. The first example above, the equivalent conductivity pore radius, pointed out a problem in the exit rate; at 0.1 M , near the saturation level of the SR channel, the measured channel conductance is higher than that of a 1-nm diameter pore of 5 nm length governed by homogeneous aqueous diffusion. Here, it is the maximum conductance that is "too high." The second and third examples point out a problem with the *entry* rate: that it appears to be much higher than the rate of diffusion up to an opening of a reasonable radius of 0.2 nm or less. What options have we in order to resolve these problems? Let us consider each of the two rate processes separately.

Rate of Exit from the Channel, γ_{max}. One way which has been previously proposed as a means of increasing the exit rate is to design the channel such that it can accommodate several ions [6, 87]. In such a model, an ion in a singly occupied channel would have a normal, "slow" rate of leaving, but the entry into the channel of a second ion would provide an electrostatic force on the first ion, effectively decreasing its energy barrier for exit. In other words, the second ion pushes the first ion out of the channel. While this mechanism provides a possible way of raising the saturation level of conductance above simple expectations, it is not easy to calculate the magnitude of such an effect, especially since the channel structure is unknown; nor do we have any good empirical model in which the effect operates in a known way. Furthermore, both the SR and TT channels behave in a way which suggests that they may never accommodate more than one ion at a time.

The only other way (short of arbitrarily declaring a higher diffusion coefficient inside the channel than in free solution) of increasing the maximum conductance is to postulate that the physical length along which the channel-mediated restricted diffusion takes place is shorter than the 50 Å assumed in example 1. While it is unreasonable to postulate that the total length of an integral membrane-spanning protein is much shorter than this, we could easily imagine a channel structure in which the restricted diffusion occurs along a *short* constriction connected to the external solutions *via* wide mouths. Returning to the naive homogeneous diffusion example, a pore of length 1 nm and SR-channel conductance 130 pS at 0.1 M KCl would have a calculated radius of 0.18 nm, now in a range which would allow selectivity. A similar calculation for the TT channel, which has a conductance of 230 pS in 0.1 M KCl, would lead to an equivalent pore of 1 nm in length and 0.24 nm in radius. Thus, by reducing the length of the channel's constriction, we can increase the maximum conductance to an acceptable range.

Rate of Entry into the Channel, γ_{max}/K_d. Decreasing the length of the channel will be of no help in removing the problem of diffusion limitation up to the channel opening. Examination of Eq. (12) shows that there is only one way to do this: to increase the channel's capture radius; i.e., to make a larger area available to the external solution for capture of an ion by the channel. It might be imagined that the wide mouths postulated above to exist on the two sides of the channel would serve this function, but this is not the case. The mouths were invoked in order to reduce the length of the channel proper, i.e., the length of the region of the protein in which restricted diffusion takes place. Therefore, by definition, normal unrestricted aqueous-like diffusion occurs within the mouths, up to the beginning of the short constriction, and the constraints of diffusion-limitation to entry must apply there as well. Thus, the wide mouths serve only to increase the maximum conductance; they cannot increase the entry rate.

We are left in a problematical situation, then, to explain these high rates of K^+ entry into the channels. We must increase the capture area of the channel, but we cannot simply expand the channel's bore, as we would necessarily lose selectivity. The way out of the problem is to increase the radius of the pore, but then to allow a constriction to occur within the channel, a region at which the critical ion-selectivity mechanism is placed; i.e., a classical "selectivity filter." In this way, the capture area exposed to the aqueous diffusion region may remain large, but selectivity will be possible because of the narrowing of the pore (Fig. 4).

The question arises in such a structure, why isn't the narrowest constriction of the pore, the selectivity filter, taken as the capture area? Why

are we permitted to use the wider opening which the "short tunnel" presents to the aqueous diffusion region? In what way is the wider part of the short tunnel any different from the wide mouths, which we have already rejected as a mechanism for increasing the entry rate? These are central questions. The difference between the wide mouths and the lumen of the short tunnel is that the applied voltage is assumed to drop *only* along the tunnel. In this region, normal aqueous diffusion does *not* occur; instead, the single-ion rule of the channel applies. Thus, in the mouth of the channel, the ion must diffuse randomly until it is captured by the short tunnel. Once inside the tunnel, the ion may now be swept through the channel by the applied electric field; it does not need to "collide" randomly with the narrower selectivity filter.[5]

Conclusions

The present survey of K^+ channels leads to the generalization that the conducting pathways of all of these channels are built along the same overall plan. In all cases, K^+ (or Tl^+) is the most conductive ion, and in no case does Cs^+ show measurable conductance; selection of K^+ over Na^+ is always good to exquisite. These results lead to models of the channel as containing constrictions, or selectivity filters, at which partial dehydration of the cation must occur in exchange for liganding groups on the channel protein. According to this view, Na^+ cannot permeate because its dehydrated form cannot interact fully with the selectivity filter, while the hydrated form is excluded sterically; likewise, the dehydrated Cs^+ ion, though perhaps able to bind well to the filter, would be too large to permeate. The rigidities of the selectivity filters of the various K^+ channels may be vastly different; the filters of the highly selective channels such as the maxi K^+ TT channel and the inward rectifier, which discriminate K^+ even from Rb^+, are pictured as precisely fitting the K^+ ion, with very little "play" in the fit. On the other extreme, the constriction in the SR channel would be wider and flexible enough to allow even Li^+ ion through to a small extent.

In all cases examined, experiments with blocking molecules have required the postulation of large access regions, or "mouths," on one or both sides of these channels. In most cases, these mouths appear to contain hydrophobic areas, a somewhat surprising structural feature to be found in an essentially hydrophilic pore. We think it unlikely that these hydrophobic regions represent the hydrocarbon phase of the lipid bilayer; rather, it is easiest to imagine them as "cracks" in the otherwise hydrophilic wall of the protein, low-dielectric cracks which the physiological metal cations avoid entering.

Considering the above similarities in K^+ channel models, we should ask why there exist two clearly separated classes of K^+ channels: low-conductance channels, such as the delayed rectifier, and high-conductance maxi K^+ channels. What is the essential difference between these two channel types? In the absence of hard structural data, we cannot answer this question. But we can offer a speculative hypothesis to explain this difference, a hypothesis which is economical if nothing else. As in Figs. 1 and 4, we view these channels as containing three regions: a mouth or mouths in which unrestricted diffusion occurs, a "tunnel" along which the applied voltage drops, and a selectivity filter within the tunnel. *We propose that the two types of K^+ channels differ primarily in the physical lengths of the tunnel regions.* Maxi K^+ channels are pictured to have short tunnels, while the small K^+ channels have long tunnels.

In only a single case has a concerted attempt been made to place a length on a channel's tunnel:

[5] Another way of increasing the area of the channel's entryway would be to postulate that the channel is actually made up of multiple diffusion pathways in parallel, embedded in the same protein complex, and all gating together – a "Gatling gun" structure. If each of the barrels of the gun acts as a single-ion channel, and if they all open and close together, then the collection of channels will follow the single-ion behavior followed by each one. Of course, ionic selectivity could be maintained, since *each* separate diffusion pathway would have a small channel conductance of, say, 10 pS. It is also necessary to realize that for such a picture to work, the individual barrels would have to be separated by enough distance so that each one "sees" an aqueous diffusion region which does not overlap with the aqueous regions seen by any other barrel. To avoid significant interaction among the individual access regions, the barrels would have to be separated by distances substantially greater than the channel diameter [86]; i.e., by several Å.

This may seem to be an outrageously unlikely structure, but there is very little direct evidence to rule it out. The only extant observation arguing against the model concerns the blocking of the SR K^+ channel by bis-quaternary ammonium compounds such as decamethonium and its analogues. These compounds induce "flickering" on the open SR channel, and a detailed study [102] has provided strong evidence that each downward transition represents the entry of a single molecule of the blocker into the K^+ diffusion pathway of the channel. Now, it is difficult to see how a single decamethonium molecule would be able simultaneously to plug, say, 10 diffusion pathways of a Gatling gun structure. This type of flickering behavior argues, at least for the SR channel, that the K^+ current through the channel occurs in a single diffusion pathway. (That a channel might operate by a structure with several diffusion pathways gating together is not *a priori* unlikely; indeed, such a model, with *two* such coupled diffusion pathways, has been proposed to explain the fast-gating behavior of the Cl-specific channel from *Torpedo* electroplax [106].)

that of the SR channel [33, 102–104]. The physical dimensions inferred from blocking and ion-water flux coupling in this channel are shown in Fig. 4. Here, the tunnel is postulated to be wide (0.6–0.7 nm diameter), and short (1 nm in length). The width of the tunnel would explain the high K^+ entry rate, while its shortness would account for the large maximum conductance of the channel. Hemocyanin appears to conform to this picture as well [23, 24]. According to the analysis of high-conductance channels above, we think it likely that a similar picture will emerge for the Ca^{2+}-activated maxi K^+ channels. We would also explain the low conductances of the delayed and inward rectifiers as a manifestation of a longer tunnel region; this tunnel may not be as wide as 0.6–0.7 nm, but it still must be able to accommodate the TMA ion (0.5 nm diameter) along most of its length.

One expectation of the tunnel-length hypothesis is that all maxi K^+ channels should obey the single ion rule and that small K^+ channels should show multiple ion interactions within the channel. This conclusion follows from the electrostatic ion-ion interaction energy required to place a second ion inside a channel's tunnel. Consider a channel containing two chemically identical binding sites separated by a given distance. We may use Levitt's [89] electrostatic treatment for a 0.6-nm pore to estimate that for a separation of 0.6 nm, as for the SR K^+ channel, the energy of charge-charge repulsion alone would be in the order of 17 kJ/mol. This corresponds to a binding affinity for the second ion 1,000-fold lower than that of the first ion. Thus, if the first ion binds with a dissociation constant of 50 mM (as with the SR or TT K^+ channels), the second ion will always be excluded in any attainable range of K^+ concentration. Levitt's calculations show that the ion-ion repulsion decreases rapidly as the separation increases [89]. Thus, if the binding sites are separated by 2.1 nm, as is the case for K^+ in gram A [75], the affinities of the two binding reactions would differ by only one order of magnitude; this expectation is in reasonable agreement with the measured binding constants for the two K^+ ions occupying this multi-ion channel [111]. Thus, we picture maxi K^+ channels as containing several possible K^+-binding sites, only one of which may be occupied at any time because of the small separation of the sites; low-conductance K^+ channels, with their longer tunnel regions, would not be so constrained and would tend to show multi-ion behavior. This prediction has been confirmed in all of those cases in which the question has been rigorously addressed: the SR and TT K^+ channels show especially clean single-ion behavior as does the highly conductive hemocyanin channel, and both the delayed and anomalous rectifiers display multi-ion occupancy.

Now that single-channel measurements are becoming almost routinely applicable, the time is ripe to apply several previously unfeasible tests to K^+ channels to assess the validity of the "tunnel-length" hypothesis. Most fundamentally, the variation of channel conductance with K^+ concentration should be determined, to obtain an idea of the entry rates, exit rates, and binding energies for these channels. Limiting currents at low K^+ and high voltage may be used to indicate the "access area" of the channel's tunnel [6]. An estimate for the length of the narrowest regions of the channel can be made from determinations of channel-mediated streaming potential, as has been done with gram A [91, 122], the SR K^+ channel [103], and hemocyanin [23]. Finally, the technique of mapping the electric field within a channel's ion diffusion pathway by use of divalent blockers [102] may provide an independent measurement of the tunnel length. Each of these methods is admittedly crude, but a determined assault using all of them together seems to be the only way presently available to probe ion channels in hopes of relating ion conduction function to the underlying protein structure.

We are grateful for the critical appraisals of Dr. Dale Benos, Peter Jordan, and Cecilia Vergara. We also acknowledge Miss Abigail Miller's expert assistance in the preparation of the manuscript.

This work was supported by NIH grants GM25277 and GM28992 (to R.L.) and AM-00354 (to C.M.).

References

1. Adam, G., Delbrück, M. 1968. *In*: Structural Chemistry and Molecular Biology. N. Davidson and A. Rich, editors. pp. 198–215. W.H. Freeman, San Francisco
2. Adams, P.R., Constantin, A., Brown, D.A., Clark, R.B. 1982. *Nature (London)* **296**:746–749
3. Adelman, W.J., Jr., French, R.J. 1978. *J. Physiol. (London)* **276**:13–25
4. Almers, W. 1972. *J. Physiol. (London)* **225**:57–83
5. Alvarez, O., Diaz, E., Latorre, R. 1975. *Biochim. Biophys. Acta* **389**:444–448
6. Andersen, O.S., Procopio, J. 1980. *Acta Physiol. Scand. Suppl.* **481**:27–35
7. Armstrong, C.M. 1971. *J. Gen. Physiol.* **58**:413–437
8. Armstrong, C.M. 1975. *In*: Membranes, A Series of Advances. G. Eisenman, editor. Vol. 3, pp. 325–358; Dekker, New York
9. Armstrong, C.M. 1975. *Q. Rev. Biophys.* **7**:179–210
10. Armstrong, C.M., Hille, B. 1972. *J. Gen. Physiol.* **59**:388–400
11. Armstrong, C.M., Taylor, S. 1980. *Biophys. J.* **30**:473–488

12. Barry, P.H., Gage, P.W., Van Helden, D.F. 1979. *J. Membrane Biol.* **45**:245–276
13. Bean, R.C., Shepperd, W.C., Chan, M., Eichner, J. 1969. *J. Gen. Physiol.* **53**:741–757
14. Begenisich, T., De Weer, P. 1980. *J. Gen. Physiol.* **76**:83–98
15. Begenisich, T., Stevens, C.F. 1975. *Biophys. J.* **15**:843–846
16. Benos, D.J., Mandel, L.J., Simon, S.A. 1980. *J. Gen. Physiol.* **76**:233–247
17. Benson, J.A., Levitan, I. 1983. Serotonin increases an anomalously rectifying K current in *Aplysia* neurone R15. *Proc. Natl. Acad. Sci. USA (in press)*
18. Benz, R., Hancock, R.E.W. 1981. *Biochim. Biophys. Acta* **646**:298–308
19. Bezanilla, F., Armstrong, C.M. 1972. *J. Gen. Physiol.* **60**:588–608
20. Binstock, L., Lecar, H. 1969. *J. Gen. Physiol.* **53**:342–361
21. Born, M. 1920. *Z. Phys.* **1**:45–48
22. Cecchi, X., Alvarez, O., Latorre, R. 1981. *J. Gen. Physiol.* **78**:657–681
23. Cecchi, X., Bull, R., Franzoy, R., Coronado, R., Alvarez, O. 1982. Hemocyanin channel. Probing pore size. *Biochim. Biophys. Acta (in press)*
24. Cecchi, X., Latorre, R., Alvarez, O. 1982. Hemocyanin channel. Alkaline metal ion selectivity. *Biophys. J. (submitted)*
25. Colombini, M. 1980. *J. Membrane Biol.* **53**:79–84
26. Colquhoun, D., Neher, E., Reuter, H., Stevens, C.F. 1981. *Nature (London)* **294**:752–754
27. Conti, F., DeFelice, L.F., Wanke, E. 1975. *J. Physiol. (London)* **248**:45–82
28. Conti, F., Neher, E. 1980. *Nature (London)* **285**:140–143
29. Conti, F., Hille, B., Neumcke, B., Donner, W., Stampfli, R. 1976. *J. Physiol. (London)* **262**:699–727
30. Coronado, R., Latorre, R. 1982. *Nature (London)* **298**:849–852
31. Coronado, R., Miller, C. 1979. *Nature (London)* **280**:807–810
32. Coronado, R., Miller, C. 1980. *Nature (London)* **288**:495–497
33. Coronado, R., Miller, C. 1982. *J. Gen. Physiol.* **79**:529–547
34. Coronado, R., Rosenberg, R.L., Miller, C. 1980. *J. Gen. Physiol.* **76**:425–446
35. Coronado, R., Williams, A. 1982. *Biophys. J.* **37**:343*a*
36. Dawson, C.M., Atwater, I., Rojas, E. 1982. *J. Membrane Biol.* **64**:33–43
37. Dean, P.M., Matthews, E.K. 1968. *Nature (London)* **219**:389–390
38. Dwyer, T.M., Adams, D.J., Hille, B. 1980. *J. Gen. Physiol.* **75**:469–492
39. Eaton, D.C., Brodwick, M.S. 1980. *J. Gen. Physiol.* **75**:727–750
40. Ehrenstein, G., Lecar, H., Nossal, R. 1970. *J. Gen. Physiol.* **55**:119–133
41. Eisenberg, M., Hall, J.E., Mead, C.A. 1973. *J. Membrane Biol.* **14**:143–176
42. Eisenman, G. 1961. *In*: Symposium on Membrane Transport and Metabolism. A. Kleinzeller and A. Kotyk, editors. pp. 163–179. Academic Press, New York
43. Finkelstein, A., Andersen, O.S. 1981. *J. Membrane Biol.* **59**:155–171
44. Frankenhaeuser, B., Moore, L.E. 1963. *J. Physiol. (London)* **169**:431–437
45. French, R.J., Adelman, W.J., Jr. 1976. *Curr. Top. Membranes Transp.* **8**:161–207
46. French, R.J., Shoukimas, J.J. 1981. *Biophys. J.* **34**:271–292
47. French, R.J., Wells, J.B. 1977. *J. Gen. Physiol.* **70**:707–724
48. Fukushima, F. 1981. *Nature (London)* **294**:368–371
49. Gardos, G. 1958. *Biochim. Biophys. Acta* **30**:653–654
50. Gay, L.A. 1981. *J. Physiol. (London)* **312**:39*P*–40*P*
51. Gay, L.A., Stanfield, P.R. 1977. *Nature (London)* **267**:169–170
52. Gorman, A.L.F., Woodlum, J.C., Cornwall, M.C. 1982. *Biophys. J.* **38**:319–322
53. Grinstein, S., Du Pre, A., Rothstein, A. 1982. *J. Gen. Physiol.* **79**:849–868
54. Hagiwara, S., Kidokoro, Y. 1971. *J. Physiol. (London)* **219**:217–232
55. Hagiwara, S., Miyazaki, S., Moody, N., Patlak, J. 1978. *J. Physiol. (London)* **279**:167–185
56. Hagiwara, S., Miyazaki, S., Rosenthal, N.P. 1976. *J. Gen. Physiol.* **67**:621–638
57. Hagiwara, S., Takahashi, K. 1974. *J. Membrane Biol.* **18**:61–80
58. Hall, J.E. 1975. *J. Gen. Physiol.* **6**:531–532
59. Hammill, O.P. 1981. *J. Physiol. (London)* **319**:97*P*–98*P*
60. Hammill, O.P., Marty, A., Neher, E., Sakmann, B., Sigworth, F.J. 1981. *Pfluegers Arch.* **391**:85–100
61. Hammill, O.P., Sakmann, B. 1981. *Nature (London)* **294**:462–464
62. Hermann, A., Gorman, A.L.F. 1981. *J. Gen. Physiol.* **78**:87–110
63. Hille, B. 1971. *J. Gen. Physiol.* **58**:599–619
64. Hille, B. 1973. *J. Gen. Physiol.* **61**:669–686
65. Hille, B. 1975. *In*: Membranes, A Series of Advances. G. Eisenman, editor. Vol. 3, pp. 255–323. Dekker, New York
66. Hille, B., Schwarz, W. 1978. *J. Gen. Physiol.* **72**:409–442
67. Hille, B., Schwarz, W. 1979. *Brain Res. Bull.* **4**:159–162
68. Hodgkin, A.L., Horowicz, P. 1959. *J. Physiol. (London)* **148**:127–160
69. Hodgkin, A.L., Huxley, A.F. 1952. *J. Physiol. (London)* **117**:500–544
70. Hodgkin, A.L., Keynes, R.D. 1955. *J. Physiol. (London)* **128**:61–88
71. Horn, R., Patlak, J.B. 1980. *Proc. Natl. Acad. Sci. USA* **77**:6930–6934
72. Horn, R., Stevens, C. 1980. *Commun. Mol. Cell. Biophys.* **1**:57–68
73. Jordan, P.C. 1981. *Biophys. Chem.* **13**:203–212
74. Katz, B. 1949. *Arch. Sci. Physiol.* **2**:285–299
75. Koeppe, R.E., Berg, J.M., Jodgson, K.O., Stryer, L. 1979. *Nature (London)* **279**:723–725
76. Krasne, S., Eisenman, G. 1973. *In*: Membranes, A Series of Advances. G. Eisenman, editor. Vol. 3, pp. 277–328, Dekker, New York
77. Krnjevic, K., Lisiewicz, A. 1972. *J. Physiol. (London)* **255**:363–390
78. Krueger, B.K., French, R., Blaustein, M.B., Jennings, F.W. 1982. *Biophys. J.* **37**:170*a*
79. Labarca, P., Coronado, R., Miller, C. 1980. *J. Gen. Physiol.* **76**:397–424
80. Labarca, P.P., Miller, C. 1981. *J. Membrane Biol.* **61**:31–38
81. Latorre, R., Alvarez, O. 1981. *Physiol. Rev.* **61**:77–150
82. Latorre, R., Alvarez, O., Ehrenstein, G., Espinoza, M., Reyes, J. 1975. *J. Membrane Biol.* **25**:163–182
83. Latorre, R., Ehrenstein, G., Lecar, H. 1972. *J. Gen. Physiol.* **60**:75–85
84. Latorre, R., Vergara, C., Hidalgo, C. 1982. *Proc. Natl. Acad. Sci. USA* **79**:805–809
85. Läuger, P. 1973. *Biochim. Biophys. Acta* **311**:423–441
86. Läuger, P. 1976. *Biochim. Biophys. Acta* **455**:493–509
87. Läuger, P. 1980. *J. Membrane Biol.* **57**:163–178

88. Leech, C.A., Stanfield, P.R. 1981. *J. Physiol. (London)* **319**:295–309
89. Levitt, D.G. 1978. *Biophys. J.* **22**:209–219
90. Lindemann, B., Van Driessche, W. 1977. *Science* **195**:292–294
91. Levitt, D.G., Elias, S.R., Hautman, J.M. 1978. *Biochim. Biophys. Acta* **512**:436–451
92. Lux, H.D., Neher, E., Marty, A. 1981. *Pflugers Arch.* **389**:293–295
93. Marty, A. 1981. *Nature (London)* **291**:497–500
94. McIntosh, T.J., Robertson, J.D., Ting-Beall, H.P., Walter, A., Zampighi, G. 1980. *Biochim. Biophys. Acta* **501**: 289–301
95. Meech, R.W. 1972. *Comp. Biochem. Physiol.* **42A**:493–499
96. Meech, R.W. 1978. *Annu. Rev. Biophys. Bioeng.* **7**:1–18
97. Meech, R.W., Thomas, R.C. 1980. *J. Physiol. (London)* **298**:111–129
98. Meissner, H.P., Schmelz, H. 1974. *Pfluegers Arch.* **351**:195–206
99. Menestrina, G., Antolini, R. 1981. *Biochim. Biophys. Acta* **643**:616–625
100. Methfessel, C., Boheim, G. 1983. The gating of single calcium-dependent potassium channels is described by an activation-blockade mechanism. *Eur. J. Biophys. (in press)*
101. Miller, C. 1978. *J. Membrane Biol.* **40**:1–23
102. Miller, C. 1982. *J. Gen. Physiol.* **79**:869–891
103. Miller, C. 1982. *Biophys. J.* **38**:227–230
104. Miller, C. 1982. *In*: Transport in Biological Membranes, R. Antolini, editor. pp. 99–108. Raven Press, New York
105. Miller, C. 1983. Ion channel reconstitution in planar bilayer membranes. A five-year progress report. *Comm. Cell. Mol. Biophys. (in press)*
106. Miller, C. 1982. Open-state substructure of single chloride channels from Torpedo electroplax. *Phil. Trans. R. Soc. B. (London) (in press)*
107. Miller, C., Racker, E. 1976. *J. Membrane Biol.* **30**:283–300
108. Myers, V.B., Haydon, D.A. 1972. *Biochim. Biophys. Acta* **274**:313–322
109. Neher, E., Sakmann, B. 1976. *Nature (London)* **260**:799–802
110. Neher, E., Stevens, C.F. 1977. *Annu. Rev. Biophys. Bioeng.* **6**:345–381
111. Neher, E., Sandblom, J., Eisenman, G. 1978. *J. Membrane Biol.* **40**:97–116
112. Nelson, R., Arholt, R., Lindstrom, J., Montal, M. 1980. *Proc. Natl. Acad. Sci. USA* **77**:3057–3061
113. Neumcke, B., Schwarz, W., Stampfli, R. 1980. *Pfluegers Arch.* **387**:9–16
114. Ohmori, H. 1978. *J. Physiol. (London)* **281**:77–99
115. Ohmori, H. 1981. *J. Physiol. (London)* **311**:289–305
116. Ohmori, H., Yoshida, S., Hagiwara, S. 1981. *Proc. Natl. Acad. Sci. USA* **78**:4960–4964
117. Pallotta, B.S., Magleby, K.L., Barrett, J.N. 1981. *Nature (London)* **293**:471–474
118. Palmer, L.G. 1982. *J. Membrane Biol.* **67**:91–98
119. Parsegian, A. 1969. *Nature (London)* **221**:844–846
120. Patlak, J., Gration, K.A.F., Usherwood, P.N.R. 1979. *Nature (London)* **278**:643–645
121. Reuter, H., Stevens, C.F. 1980. *J. Membrane, Biol.* **57**:103–121
122. Rosenberg, P.A., Finkelstein, A. 1978. *J. Gen. Physiol.* **72**:327–340
123. Sakmann, B., Boheim, G. 1979. *Nature (London)* **282**:336–339
124. Schindler, H., Rosenbush, J.P. 1978. *Proc. Natl. Acad. Sci. USA* **75**:3751–3755
125. Schwarz, W., Neumke, B., Palade, P.T. 1981. *J. Membrane Biol.* **63**:85–92
126. Sigworth, F.J., Neher, E. 1980. *Nature (London)* **287**:447–449
127. Spalding, B.C., Senyk, O., Swift, J.G., Horowicz, P. 1981. *Am. J. Physiol.* **241**:C68–C75
128. Standen, N.B., Stanfield, P.R. 1978. *J. Physiol. (London)* **280**:169–191
129. Standen, N.B., Stanfield, P.R. 1979. *J. Physiol. (London)* **294**:497–520
130. Standen, N.B., Stanfield, P.R. 1980. *J. Physiol. (London)* **304**:415–435
131. Stanfield, P.R. 1970. *J. Physiol. (London)* **209**:231–256
132. Swenson, R. 1982. *J. Gen. Physiol.* **77**:255–271
133. Ussing, H.H. 1949. *Acta Physiol. Scand.* **19**:43–56
134. White, M., Miller, C. 1979. *J. Biol. Chem.* **254**: 10161–10166
135. Wong, B.S., Lecar, H., Adler, M. 1982. *Biophys. J.* **39**:313–317
136. Woodhull, A.M. 1973. *J. Gen. Physiol.* **61**:687–708
137. Yau, K.W., McNaughton, P.A., Hodgkin, A.L. 1981. *Nature (London)* **292**:502–505
138. Yellen, G. 1982. *Nature (London)* **296**:357–359

Received 26 July 1982

Note Added in Proof

Recently, Jordan (*Biophys. J.* **39**:157–164, 1982) has provided an exact electrostatic treatment of a cylindrical hydrophilic pore embedded in a membrane of low dielectric constant. One important result of this work is that for a channel of finite length, part of the applied transmembrane voltage falls in the aqueous regions near the pore's entryway. This effect becomes increasingly pronounced as the pore's length-to-radius ratio decreases. For a short, wide channel, as much as 40% of the voltage drop can occur in the aqueous phases, solely as a result of the polarization charge distribution in this particular geometry.

The existence of such external applied fields in short channels bears directly on several points discussed here. First, the effect raises the possibility that a blocker may show a weak voltage dependence without actually entering the channel; this may be the situation for TEA block of the delayed rectifier (p. 17). Second, the external fields would lead to an overestimate of a channel's length by the method of bis-quaternary blockers, as applied to the SR K^+ channel (p. 21). Finally, applied fields external to a channel's "tunnel" region (Fig. 4) would serve to increase the capture radius [Eq. (12)]; furthermore, the lines of force will diverge outside such a tunnel, and will, therefore, enhance an ion's entry rate into the channel by providing an electrodiffusional force in the *radial* direction. In other words, the external applied fields act as an electrostatic focusing mechanism to draw ions from the pore's mouth into the tunnel region.